Samaneh Ranjbar [a] **, M. R. Rajesh Menon** [a]**, P. A. Fernandes** [a,b] **and A. F. da Cunha**[a]

[a] *I3N- Departamento de Física, Universidade de Aveiro, Campus Universitário de Santiago, 3810-193 Aveiro, Portugal.*

[b] *Departamento de Física, Instituto Superior de Engenharia do Porto, Instituto Politécnico do Porto, Rua Dr. António Bernardino de Almeida, 431, 4200-072 Porto, Portugal.*

Effect of selenization conditions on the growth and properties of $Cu_2ZnSn(S,Se)_4$ thin films

Key: C35U1

Effect of selenization conditions on the growth and properties of $Cu_2ZnSn(S,Se)_4$ thin films

Samaneh Ranjbar [a,*] , M. R. Rajesh Menon [a], P. A. Fernandes [a,b] and A. F. da Cunha[a]

[a] *I3N- Departamento de Física, Universidade de Aveiro, Campus Universitário de Santiago, 3810-193 Aveiro, Portugal.*

[b] *Departamento de Física, Instituto Superior de Engenharia do Porto, Instituto Politécnico do Porto, Rua Dr. António Bernardino de Almeida, 431, 4200-072 Porto, Portugal.*

Abstract

The Opto-electronic properties of Copper Zinc Tin Sulfide can be tuned to achieve better cell efficiencies by controlled incorporation of selenium. In this paper we report the growth of $Cu_2ZnSn(S,Se)_4$ (CZTSSe) using a hybrid process involving the sequential evaporation of Zn and sputtering of the sulfide precursors of Cu and Sn, followed by a selenization step. Two approaches for selenization were followed, one using a tubular furnace and the other using a rapid thermal processor. The effects of annealing conditions on the morphological and structural properties of the films were investigated. Scanning electron microscopy and Energy dispersive spectroscopy were employed to investigate the morphology and composition of the films. Structural analyses were done using X-Ray Diffraction (XRD) and Raman spectroscopy. Structural analyses revealed the formation of CZTSSe. This study shows that regardless of the selenization method a temperature above 450 °C is required for conversion of precursors to a compact CZTSSe layer. XRD and Raman analysis suggests that the films selenized in the tubular

---

[*] Corresponding author; Tel: +351 234 370 200, Fax: +351 234 378 197, E-mail: samaneh.ranjbar@ua.pt

furnace are selenium rich whereas the samples selenized in the rapid thermal processor have higher sulfur content.

Keywords:

CZTSSe thin film, Tubular furnace, Rapid Thermal Processor.

1. Introduction

The light absorber photovoltaic material, Cu_2ZnSnS_4 (CZTS) has received great deal of attention in recent years due to its outstanding properties. This p-type semiconductor has high absorption coefficient above 10^4 cm^{-1} in the visible range of light and has band gap energy around 1.5 eV [1, 2]. Having these characteristics, a CZTS-based solar cell is theoretically capable of reaching an efficiency of 34% under AM 1.5 illumination, according to Shockley-Queisser calculation [3]. In addition one important advantage of CZTS compared to other absorber layers in thin film solar cell (TFSC) technology is its earth abundant and non-toxic composition, which makes it a potential cost effective and environmentally benign candidate for future TFSCs. To achieve this goal, tuning optical and electrical properties of the material are required since the best experimental conversion efficiency reported so far are below 10% for pure CZTS based solar cells and there is still a huge gap between theoretical and practical results [4]. Recent studies indicate an improvement by incorporation of Se in CZTS so as to form $Cu_2ZnSn(S_x,Se_{1-x})_4$ alloy, known as CZTSSe [5, 6, 7]. The variation of sulphur to selenium ratio in this compound changes the structural, electrical and optical properties of the film [8]. The best efficiency recorded so far for a TFSC employing CZTSSe having a $[S]/([S]+[Se])$ ratio of about 30% is 12.6% [9].

The ultimate goal of our study is to investigate the effects of selenization conditions on the structural and morphological properties of CZTSSe thin films. CZTSSe thin film is prepared using a vacuum based technique in two steps, first the deposition of $Zn/SnS_2/CuS$ precursors on the Mo-coated glass using a hybrid sputtering-evaporation technique and then annealing in a Se environment. The selenization was performed using two different approaches including tubular furnace and rapid thermal processor. The annealing conditions were varied and their effects on the film properties were studied.

2. Experimental details

$Cu_2ZnSn(S,Se)_4$ (CZTSSe) thin films are prepared in two steps. In the first step Zn was evaporated on Mo-coated glass and then SnS_2 and CuS were sputtered subsequently using an RF magnetron system. The deposition was carried out in an Ar atmosphere, at an operating pressure of 4.0×10^{-3} mbar. The process was repeated in eight periods to prepare multi-stacked layers of precursors $Zn/SnS_2/CuS$. In the second step, the precursors were selenized using two different approaches- one using a conventional Tubular Furnace (TF) and the other using a Rapid Thermal Processor (RTP). In the first approach precursors were selenized by placing them inside a graphite box within the TF, along with 140 mg of selenium pellets (99.999% purity). The pressure inside the graphite box was kept constant during the annealing at 600 mbar using N_2 gas. The precursors were selenized at various temperatures including: 350, 400, 450, 480 and 500 ^{o}C for 5 min and then cooled down naturally. In the second approach, about 2 µm thick layer of Se was deposited over identical precursor stacks after which they were annealed in an RTP furnace using N_2 + 5 % H_2 gas at a pressure of 1 atm. The heating rate and annealing time in this case were fixed at 1 K/s and 2 min, respectively. Similar to the TF approach, the precursors were annealed at maximum annealing temperatures of 400, 450, 500 and 525 ^{o}C. The morphology and the composition of the films were investigated by scanning electron microscopy (SEM) and energy dispersive spectrometry (EDS), using a SU-70 Hitachi combined with a Rontec EDS system, and the acceleration voltages of 4 kV and 25 kV were used for cross-sectional SEM and

EDS, respectively. The structural analysis was done using X-ray diffraction (XRD) and Raman spectroscopy. X-ray diffraction patterns were acquired using an XPert MPD Philips diffractometer in the Bragg–Brentano configuration (θ–2θ), using the Cu-Kα line (λ = 1.5406 Å), with the generator settings, 40 mA and 45 kV. Raman measurements were performed in the backscattering configuration using a Lab Ram Horiba HR800 UV spectrometer. Samples were excited using a laser line at 532 nm and the spectrometer is equipped with an Olympus microscope with a 100× magnification lens. The samples are named according to the type of selenization method and their maximum temperature. For example, sample selenized using TF at 500 ^{o}C was named as Se-TF-500 and that using RTP at 500 ^{o}C was named as Se-RTP-500.

3. Results and discussion

3.1 Morphological analysis

The cross-sectional SEM images of CZTSSe films selenized using the tubular furnace are shown in Fig.1a to Fig.1d. The multilayer structure of Se-TF-350 (Fig.1a) is related to the initial precursor stack, indicating that a selenization temperature of 350 ^{o}C is not enough for the full conversion of the precursors to CZTSSe. It could be observed that the grain size increased as the selenization temperature is increased. At 500 ^{o}C the grain size is about 1 µm and the film morphology has improved compared to that at lower temperatures. The composition of the samples was measured by EDS and the results are given in Table 1.

Compared to TF annealed samples, RTP annealed films were found to be more uniform and smoother. Fig.1e corresponds to the cross-sectional SEM image of the sample Se-RTP-400. It may be noted that the surface of sample consists of crystal like formations with well-defined facets. These structures are copper selenide phases and were confirmed by Raman and XRD measurements which are presented in section 3.2. On increasing the temperature to 450 ^{o}C, these well-defined crystalline structures become globular like formations (see Fig.1f) and finally it disappears completely at 525 ^{o}C (see Fig.1h). As with the samples annealed using tubular furnace, the EDS measurements revealed that the RTP annealed samples were also copper and zinc rich (see Table 1). This is evident from the presence of copper selenide crystals present over the sample surface. Similar to that observed in SEM images of the TF annealed samples, in case of RTP annealed samples also, a critical annealing temperature (450 ^{o}C) is observed, below which the precursor stack does not inter-diffuse completely to form a compact film of CZTSSe.

3.2 Structural characterization

Fig.2a shows XRD pattern of the TF annealed films under different selenization temperatures. The films annealed at 450 ^{o}C and above, show strong peaks corresponding to (112), (220), (204), (312) and (116) planes of tetragonal CZTSe, according to the International Center for Diffraction Data (ICDD), (Reference code: 04-010-6295). These results suggest that at temperatures above 450 ^{o}C all the sulfur contained in the precursor is replaced by the selenium supplied by the atmosphere during the annealing. For the films annealed at temperatures below 450 ^{o}C, there is a shift to higher diffraction angles. Considering the amount of peak shift with respect to that of pure CZTSe (27.16^{o} for (112) peak), the $[S]/([S]+[Se])$ ratio estimated using the empirical relation employed by Salome et al. [10] was 10% and 78%, respectively for Se-TF-400 and Se-TF-350. The existence of CuSe (Ref code: 01-086-1239 and 00-034-0171) is also indicated by XRD.

XRD patterns of the RTP annealed samples are given in Fig.2b. In case of RTP annealed samples also, estimation of Se incorporation was done by identifying the amount of shift in diffraction peak (112) in the XRD pattern. For the Se-RTP-400, this peak is at 27.87^{o} which is at a considerably higher (lower) position than that of pure CZTSe (CZTS) (2θ=27.16^{o}; ICDD card no. 04-010-6295 for CZTSe and 2θ=28.44°; ICDD card no.01-080-8225 for CZTS). This is clearly an indication of the formation of CZTSSe. With increase in selenization temperature, the peak slowly shifts to lower values suggesting that more and more Se is being incorporated. The estimated ratio of $[S]/([S]+[Se])$ is given in Table 2. In addition to the main peaks, peaks corresponding to the secondary phases are also observed in the diffraction pattern. For Se-RTP-400 a secondary peak could be seen at a diffraction angle of 31.45°. This could be due to either CuSe (2θ=31.11°; ICDD card no.01-086-1239) or due to SnS (2θ=31.52°; ICDD card no. 04-004-3833); or may be due to both. Presence of CuSe is evident from the cross-sectional SEM images whereas that of SnS may be justified from the fact that the layers of precursors are not completely inter-diffused at this temperature (see Fig.1e) and that SnS_2 might have decomposed to SnS. The variation of (112) peak position and crystallite size with annealing temperature for TF and RTP annealed samples is given in Table 2. The crystallite size was evaluated from the XRD data using the Scherrer formula.

Fig.3a shows the Raman spectra of TF annealed samples. Raman spectra of the samples annealed at 450 °C and higher temperatures has characteristic peaks at 173, 196, 235 cm^{-1} indicating the formation of pure CZTSe [10]. The samples annealed at lower temperatures shows a bimodal behavior in the Raman spectrum with peaks corresponding to A1 vibrational modes of CZTSe and CZTS. However, the A1 mode vibrations of CZTSe are shifted to higher wavenumbers whereas that of CZTS is shifted to lower wavenumbers. This clearly is an indication of the formation of a CZTSSe phase in which S atoms are partially replaced by Se. The intense peak in case of Se-TF-350 is at 333 cm^{-1} indicating the presence of CZTSSe, the other peak at 235 cm^{-1} may be related to CZTSe. Se-TF-400 has a small peak at 328 cm^{-1} that indicates the presence of CZTSSe, it also has an intense peak at 196 cm^{-1} corresponding to CZTSe and a shoulder at 202

cm^{-1} that may correspond to a CZTSSe phase with an estimated $[S]/([S]+[Se])$ ratio of 15% [10]. The peaks in the range 260-267cm^{-1} in the spectra belong to CuSe phase.

Raman spectra of RTP annealed films at 400 and 450 ^{o}C consist of two broad peaks centered at 215 and 330.5 cm^{-1} (see Fig.3b). However, it may be noted that the peak at 215 cm^{-1} is actually composed of two peaks one centered around 211cm^{-1} and the other at around 220.5 cm^{-1}. The peak at 211 cm^{-1} appears only as a shoulder to the peak at 220.5 cm^{-1} in Se-RTP-400. On increasing the annealing temperature to 450 ^{o}C, the intensity of this peak increases, indicating its association with CZTSe, since it is likely that more sulfur is being replaced by selenium with an increase in temperature. On the other hand, the relative intensity of the peak at 220.5 cm^{-1} remains unchanged and its origin is unknown. The peak at 330.5 cm^{-1} is attributed to CZTSSe. At higher temperatures, this peak is almost completely suppressed and the spectra consist of only three peaks at 174, 197 and 234.5 cm^{-1} characteristic of CZTSe.

4. Conclusions

The effect of selenization temperature on the structural and morphological properties of CZTSSe thin films obtained through the selenization of multi-stacked precursors using a conventional tubular furnace (TF) and a rapid thermal processor (RTP) was studied. From the cross-sectional SEM analysis, it was observed that at temperatures lower than 450 ^{o}C, irrespective of the selenization method, the precursor stack does not inter-diffuse completely to form a compact layer of CZTSSe. The film formed at these temperatures consists of a sulfur rich CZTSSe phase along with secondary phases of CuSe and SnS. At 450 ^{o}C, sulfur in the precursors is almost completely replaced by selenium in the conventional tubular furnace where as in RTP a much higher percentage of sulfur is observed. Above 450 ^{o}C, RTP selenization also resulted in Se rich films. However, the results suggest that RTP selenization method could have some advantages over the conventional tubular furnace in obtaining smooth, uniform and compact films of CZTSSe at much shorter selenization time, they also point to the fact that a minimum annealing temperature of 450 °C is essential for obtaining compact films.

Acknowledgements

Samaneh Ranjbar thanks the financial support of the Portuguese Science and Technology Foundation (FCT) through PhD grant SFRH / BD / 78409 / 2011. M. R. Rajesh Menon acknowledges the financial support provided through the project “Harvesting the energy of the sun for a sustainable future”, Projeto 07/ST24/FEDER/002032 (CENTRO). FCT is also acknowledged for supporting this work through the grants PTDC/CTM-MET/113486/2009, PEST-C/CTM/LA0025/2011and RECI/FIS-NAN/0183/2012.

References

[1] H. Katagiri, K. Jimbo, W. S. Maw, K. Oishi, M. Yamazaki, H. Araki, A. Takeuchi, Development of CZTS-based thin film solar cells, Thin Solid Films 517 (2009) 2455-2460.

[2] J. P. Leitão, N. M. Santos, P. A. Fernandes, P. M. P. Salomé, A. F. da Cunha, J. C. González, F. M. Matinaga, Study of optical and structural properties of Cu_2ZnSnS_4 thin films, Thin Solid Films 519 (2011) 7390-7393.

[3] W. Ki, H. W. Hillhouse, Earth-Abundant Element Photovoltaics Directly from Soluble Precursors with High Yield Using a Non-Toxic Solvent, Adv. Energy Mater. 1 (2011) 732-735.

[4] M. A. Green, K. Emery, Y. Hishikawa, W. Warta, E. D. Dunlop, Solar cell efficiency tables (version 43), Prog. Photovolt: Res. Appl. 22 (2014) 1-9.

[5] K. Woo, Y. Kim, W. Yang, K. Kim, I. Kim, Y. Oh, J. Y. Kim, J. Moon, Band-gap-graded $Cu_2ZnSn(S_{1-x},Se_x)_4$ Solar Cells Fabricated by an Ethanol-based, Particulate Precursor Ink Route, Sci. Rep. 3 (2013) 3069-3075.

[6] M. T. Winkler, W. Wang, O. Gunawan, H. J. Hovel, T. K. Todorova, D. B. Mitzi, Optical designs that improve the efficiency of $Cu_2ZnSn(S,Se)_4$ solar cells, Energy Environ. Sci. 7 (2014) 1029-1036.

[7] S. W. Shin , I. Y. Kim , K.V. Gurav , C. H. Jeong , J. H. Yun, P. S. Patil, J. Y. Lee , J. H. Kim, Band gap tunable and improved microstructure characteristics of $Cu_2ZnSn(S_{1-x},Se_x)_4$ thin films by annealing under atmosphere containing S and Se, Curr. Appl. Phys. 13 (2013) 1837-1843.

[8] S. Chen, A. Walsh, J.-H. Yang, X. G. Gong, L. Sun, P.-X. Yang, J.-H. Chu, S.-H. Wei, Compositional dependence of structural and electronic properties of $Cu_2ZnSn(S,Se)_4$ alloys for thin film solar cells, Phys. Rev. B 83 (2011) 125201-125205.

[9] W. Wang , M. T. Winkler , O. Gunawan , T. Gokmen , T. K. Todorov , Y. Zhu , D. B. Mitzi, Device Characteristics of CZTSSe Thin-Film Solar Cells with 12.6% Efficiency, Adv. Energy Mater. 4 (2014), 1301465-1301469.

[10] P. M. P. Salomé , J. Malaquias, P. A. Fernandes, M. S. Ferreira, A. F. da Cunha, J. P. Leitão, J. C. González , F. M. Matinaga, Growth and characterization of $Cu_2ZnSn(S,Se)_4$ thin films for solar cells, Sol. Energy Mater. Sol. Cells 101 (2012) 147-153.

Table 1. Metal composition of the samples at various temperatures.

Sample	[Cu]/[Zn]	[Cu]/[Sn]	[Zn]/[Sn]	[Cu]/([Zn]+[Sn])
Se-TF-350	2.66	2.31	0.87	1.24
Se-TF-400	2.03	1.9	0.93	0.98
Se-TF-450	1.34	2.02	1.51	0.81
Se-TF-480	2.04	3.5	1.71	1.29
Se-TF-500	2.27	3.23	1.42	1.33
Se-RTP-400	1.95	3.56	1.82	1.26
Se-RTP-450	1.95	2.99	1.53	1.18
Se-RTP-500	1.76	2.77	1.57	1.08
Se-RTP-525	1.77	2.72	1.53	1.07

Table 2. (112) peak position, Full Width at Half Maximum (FWHM) and crystallite size of samples selenized in a tubular furnace (TF) and a rapid thermal processor (RTP) at various temperatures.

Selenization Temperature (^{o}C)	**(112) peak position (degree)**	**FWHM (degree)**	**Crystallite size (nm)**	$\frac{[S]}{([S]+[Se])}$ **(%)**
Se-TF-350	28.16	0.38	21.5	78
Se-TF-400	27.30	0.30	27.2	10
Se-TF-450	27.17	0.15	54.5	< 1
Se-TF-480	27.17	0.14	58.4	< 1
Se-TF-500	27.17	0.14	58.4	< 1
Se-RTP-400	27.87	0.28	29.6	55
Se-RTP-450	27.68	0.25	33.1	41
Se-RTP-500	27.28	0.20	41.3	9
Se-RTP-525	27.25	0.18	45.9	7

Fig.1. Cross-sectional SEM images of samples selenized in a tubular furnace (TF) and a rapid thermal processor (RTP) at various temperatures: (a) Se-TF-350, (b) Se-TF-450, (c) Se-TF-480, (d) Se-TF-500, (e) Se-RTP-400, (f) Se- RTP-450, (g) Se- RTP-500 and (h) Se- RTP-525.

Fig.2. XRD patterns of samples selenized (a) using a tubular furnace (TF), and (b) a rapid thermal processor (RTP), at various temperatures.

Fig.3. Raman spectra of samples selenized (a) using a tubular furnace (TF), and (b) a rapid thermal processor (RTP) at various temperatures.

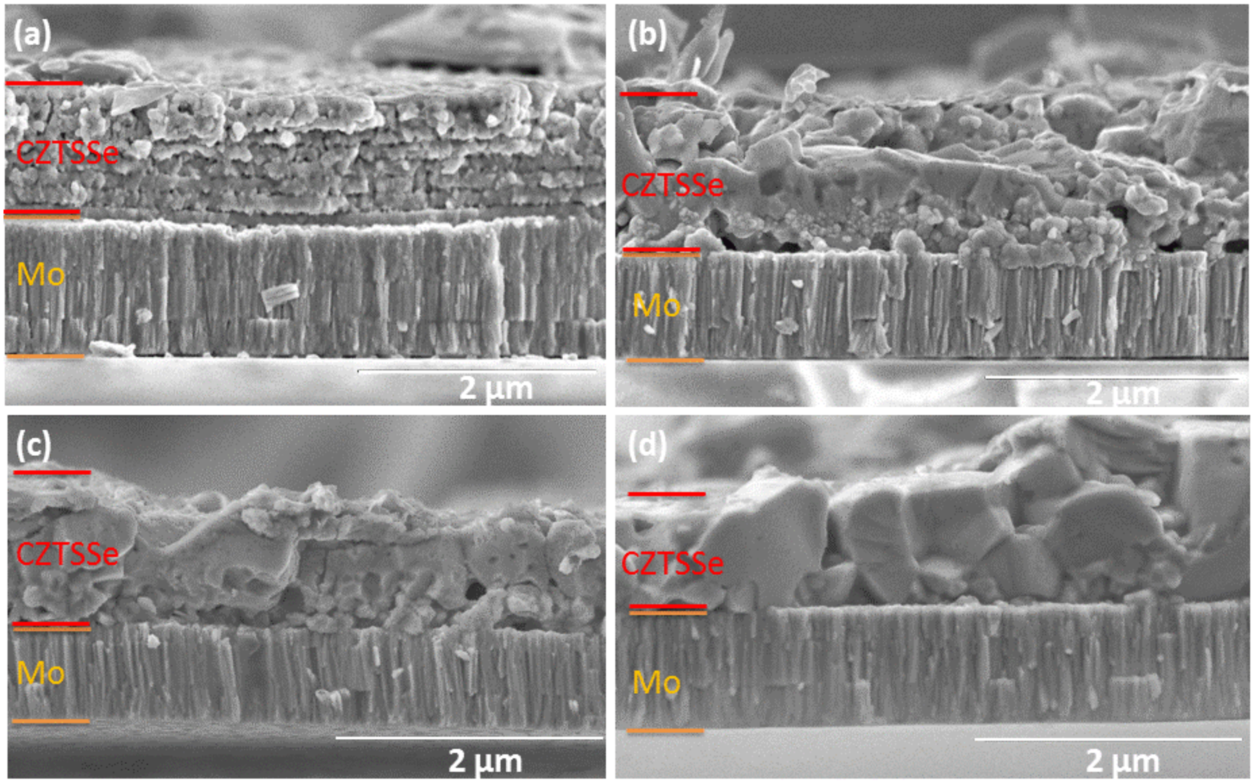
(a)
CZTSSe
Mo
2 µm
(b)
CZTSSe
Mo
2 µm
(c)
CZTSSe
Mo
2 µm
(d)
CZTSSe
Mo
2 µm

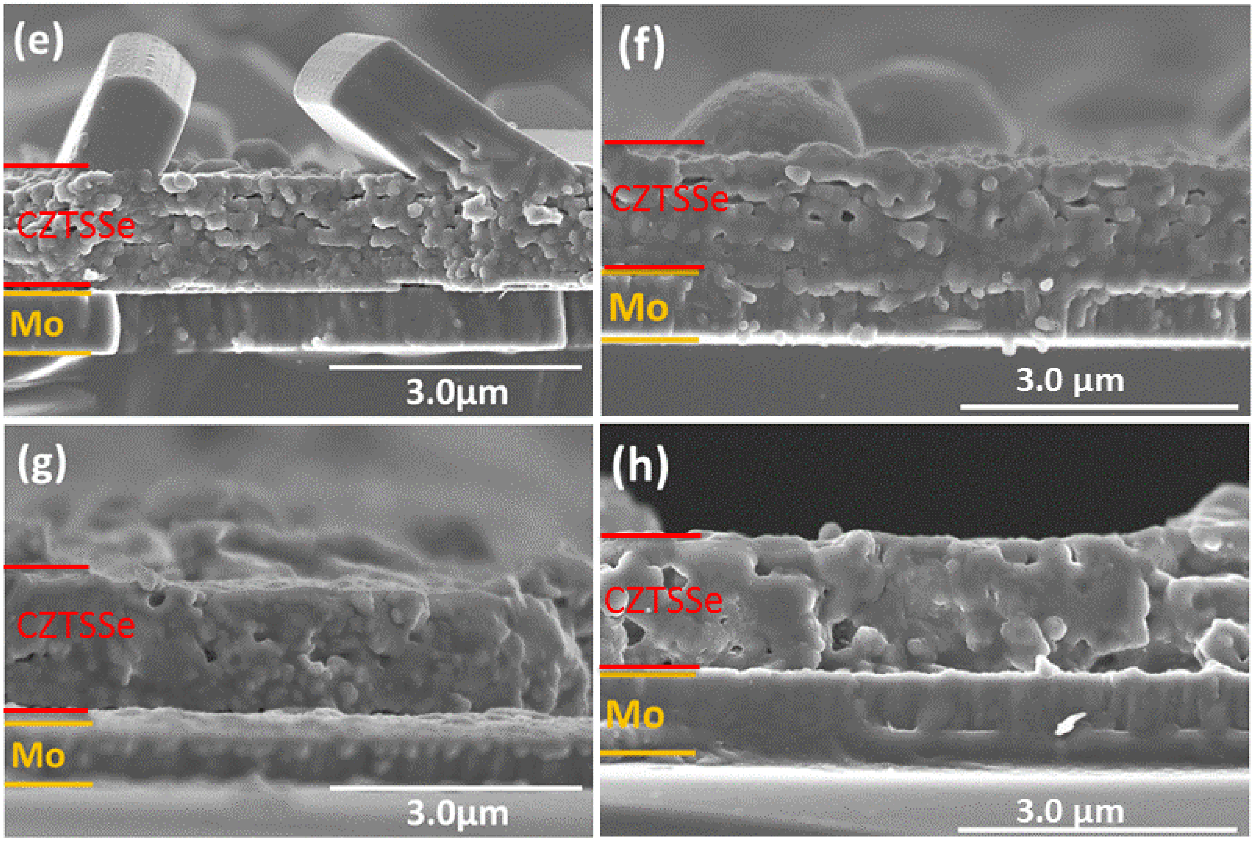
(e)
CZTSSe
Mo
3.0µm
(f)
CZTSSe
Mo
3.0 µm
(g)
CZTSSe
Mo
3.0µm
(h)
CZTSSe
Mo
3.0 µm

Fig.1.

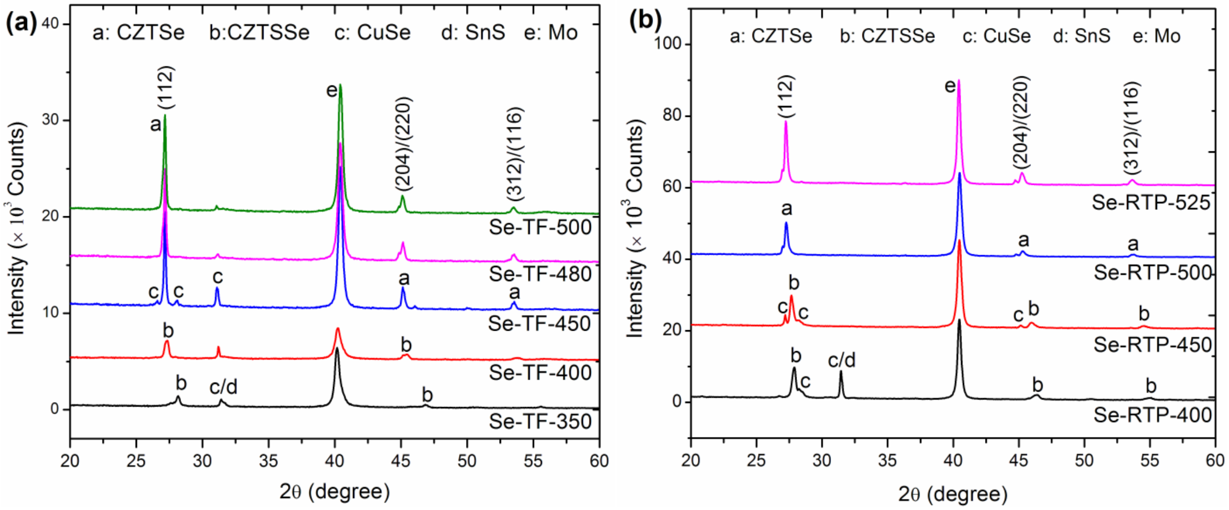
(a)
a: CZTSe
b:CZTSSe
c: CuSe
d: SnS
e: Mo
(112)
(204)/(220)
(312)/(116)
Se-TF-500
Se-TF-480
Se-TF-450
Se-TF-400
Se-TF-350
Intensity (× 10³ Counts)
2θ (degree)
0
10
20
30
40
20
25
30
35
40
45
50
55
60
(b)
a: CZTSe
b: CZTSSe
c: CuSe
d: SnS
e: Mo
(112)
(204)/(220)
(312)/(116)
Se-RTP-525
Se-RTP-500
Se-RTP-450
Se-RTP-400
Intensity (× 10³ Counts)
2θ (degree)
0
20
40
60
80
100
20
25
30
35
40
45
50
55
60

Fig.2.

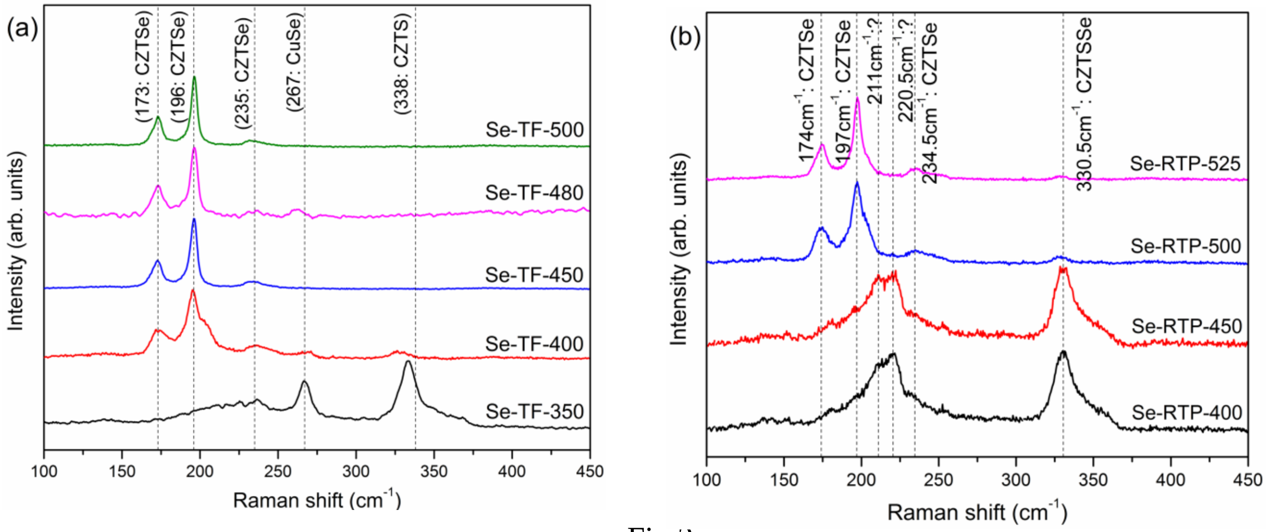
(a)
(173: CZTSe)
(196: CZTSe)
(235: CZTSe)
(267: CuSe)
(338: CZTS)
Se-TF-500
Se-TF-480
Se-TF-450
Se-TF-400
Se-TF-350
Intensity (arb. units)
100
150
200
250
300
350
400
450
Raman shift (cm^{-1})
(b)
174cm^{-1}: CZTSe
197cm^{-1}: CZTSe
211cm^{-1}:?
220.5cm^{-1}:?
234.5cm^{-1}: CZTSe
330.5cm^{-1}: CZTSSe
Se-RTP-525
Se-RTP-500
Se-RTP-450
Se-RTP-400
Intensity (arb. units)
100
150
200
250
300
350
400
450
Raman shift (cm^{-1})

Fig.3.